IEEE Access
Multidisciplinary | Rapid Review | Open Access Journal

Received April 7, 2021, accepted April 27, 2021, date of publication May 13, 2021, date of current version May 21, 2021.

*Digital Object Identifier 10.1109/ACCESS.2021.3079915*

# Design and Prototype Implementation of Software-Defined Radio Over Fiber

**TAKUMASA ISHIOKA[1], (Member, IEEE), KAZUKI AIURA[1], RYOTA SHIINA[2], TATSUYA FUKUI[2], TOMOHIRO TANIGUCHI[2], SATOSHI NARIKAWA[2], KATSUYA MINAMI[2], KAZUHIRO KIZAKI[1], TAKUYA FUJIHASHI[1], (Member, IEEE), TAKASHI WATANABE[1], (Member, IEEE), AND SHUNSUKE SARUWATARI[1], (Member, IEEE)**

[1]Graduate School of Information Science and Technology, Osaka University, Osaka 565-0871, Japan
[2]NTT Access Network Service Systems Laboratories, NTT Corporation, Tokyo 180-8585, Japan

Corresponding author: Takumasa Ishioka (ishioka.takumasa@ist.osaka-u.ac.jp)

This work was supported in part by the Japan Society for the Promotion of Science (JSPS) KAKENHI under Grant JP18H03231 and Grant JP19H01101, and in part by the NTT Access Network Service Systems Laboratories, Japan.

**ABSTRACT** Future networks require a high degree of flexibility over wide areas to enable many services that require higher quality wireless networks such as remote control of cars and remote surgery. Therefore, the network technology must combine high capacity, low latency, and flexibility. To deal with these requirements, we developed Software-Defined Radio over Fiber (SD-RoF), which is an architecture that tightly couples light and radio at a low cost. SD-RoF offers the following two key features: elastic wireless service and elastic bidirectional passthrough. The elastic wireless service provides users with access to wireless services that they need at any time in any place. The elastic bidirectional passthrough connects two remotely located points via RoF through radio waves and enables allowing for bidirectional radio communication between devices at each location. In this study, we design and prototype implementation of SD-RoF, and conduct a basic evaluation of the implemented circuit and demonstration experiments on elastic bidirectional passthrough. Through demonstration experiments, we found the feasibility and the challenges of SD-RoF. In addition, the deployment of SD-RoF, application scenarios, and operational issues are discussed.

**INDEX TERMS** Wireless access networks, radio over fiber, software-defined networks.

## I. INTRODUCTION

The development of wireless communication technology has made network-based services, like social networking services such as Twitter and Instagram, and video streaming services such as YouTube and Netflix, available from anywhere. Moreover, high-capacity video transmission such as 4K/8K and augmented reality and virtual reality (AR/VR), sensor networks, connected cars, remote healthcare using telemedicine, remote monitoring of vital data, and many other applications are being used in wireless networks. Given that such applications will become more popular in the future, it is not practical to construct a suitable network for each application. Further, there are still some issues to be solved to realize advanced remote healthcare such as remote surgery, remote control of vehicles, and three-dimensional (3D) hologram video transmission. Therefore, future networks require a high degree of flexibility to enable a variety of applications everywhere to use the network without any inconvenience.

In the past, network function virtualization (NFV) and software-defined network (SDN) have been actively discussed to construct flexible networks. As NFV/SDN develops in the future, it is expected that it will be possible to provide flexible network services to end-users on general-purpose networks. On the other hand, it is not enough to simply provide a flexible network when considering the transmission of large content expected in the future. For example, consider remote surgery with 3D images [1]. The data rate requirement for real-time 3D video is 137 Mbps–1600 Mbps, the delay requirement is less than 150 ms, and the jitter requirement is 3–30 ms. The data rate requirement for haptic feedback is 128–400Kbps, the delay requirement is less than 3–10 ms, and the jitter requirement is less than 2 ms. Considering the synchronization between video and haptic feedback, it is desirable to fulfill the data rate requirements for video transmission and the delay and jitter requirements for

The associate editor coordinating the review of this manuscript and approving it for publication was Stefano Scanzio.

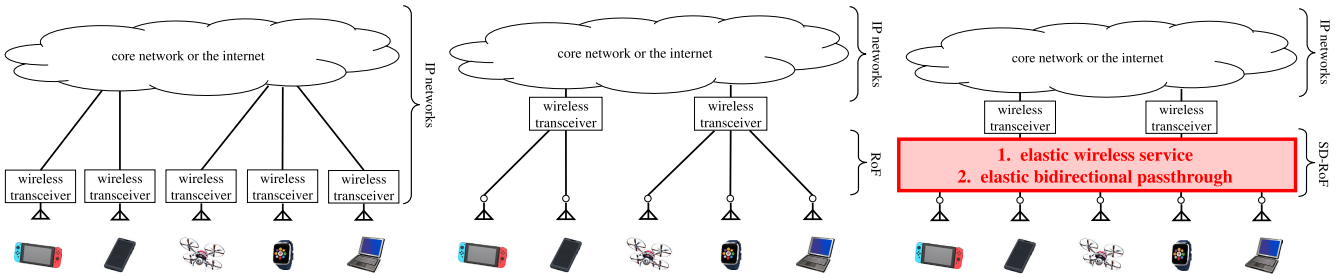


(a) Current radio access networks (b) Baseband processing-intensive radio access network such as Cloud-RAN (c) Proposed method: SD-RoF

**FIGURE 1.** Comparison of existing and proposed systems.

haptic feedback. Although increasing the performance of the network devices or suppressing latency using edge computing technology is conceivable, these methods have problems such as increased cost and reduced flexibility. Ideally, a network that combines high capacity, low latency, and flexibility should be realized at a low cost.

Given the above context, we herein propose a software-defined radio over fiber (SD-RoF) architecture. SD-RoF tightly couples optical and wireless technologies to provide a RAN with a large capacity, low latency, and protocol-free. The differences between the existing wireless access network and the proposed SD-RoF are illustrated in Figure 1. Figure 1(a) illustrates the most existing wireless access networks. The network is established using IPs, and wireless transceivers that operate as base stations are allocated at the edges to communicate with the devices. In recent years, various studies have investigated centralized wireless access networks that manage radio transceivers, such as cloud radio access networks (C-RANs), shown in Figure 1(b), to render wireless communication more flexible. Note that this paper distinguishes between wireless access networks and radio access networks because radio access networks are mainly used in cellular networks while the target of SD-RoF includes IEEE 802.11bg, Bluetooth, and IEEE 802.15.4. In SD-RoF, these wireless access networks with integrated wireless transceivers are expanded. Specifically, this enables full software control of the relationship between the antennas and wireless transceivers via networking of the RoF section of the baseband processing centralized wireless access network, as shown in Figure 1(c).

SD-RoF replaces the current IP-based wireless access network with a software-defined RoF network that combines optical and electrical switches. SD-RoF offers the following two key functions: elastic wireless service and elastic bidirectional passthrough. The elastic wireless service provides users with access to wireless services that they need at any time in any place. The elastic bidirectional passthrough connects two remotely located points via RoF through radio waves and enables bidirectional radio communication between devices at each location.

Figure 2 shows an example of SD-RoF architecture. The SD-RoF operation is described below. An SD-RoF operation

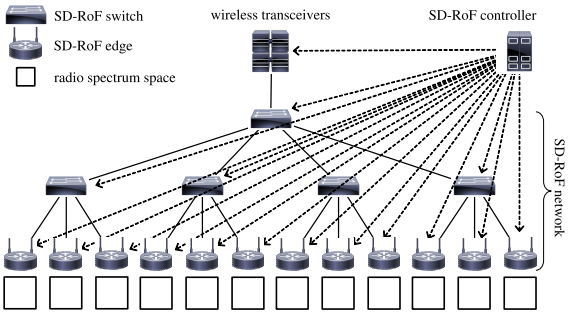


**FIGURE 2.** SD-RoF architecture.

begins when the user requests the desired wireless service from the SD-RoF controller. This request can be transmitted by setting a control channel in the SD-RoF network or by using another network, such as a cellular network. After receiving the service request, SD-RoF sends a control command to the wireless transceiver, the SD-RoF switch, and the SD-RoF edge in accordance with the request details and establishes the wireless service.

Figure 3 shows an example of an elastic wireless service. The figure shows how the SD-RoF edges communicate with wireless transceivers via the SD-RoF network and provide wireless communication services to a wireless spectrum space. In Figure 3, it provides a wireless service to radio spectrum space $\alpha$. Based on the control command from the SD-RoF controller, an RoF path is established between the wireless transceiver and SD-RoF edge $\alpha$. Because it allows users to instantly establish the necessary wireless services in any radio spectrum space, the elastic wireless service can provide the protocol-free required in next-generation radio access networks.

Figure 4 shows an example of elastic bidirectional passthrough. It connects multiple radio spectrum spaces via the SD-RoF network as if devices located in different radio spectrum spaces are directly communicating with each other. In the figure, radio spectrum spaces $\alpha$ and $\beta$ are connected via the SD-RoF network. By employing SD-RoF, three or more radio spectrum spaces can be connected. In addition, since mutually connected radio spectrum spaces can communicate directly through radio waves, broadband transmission can be

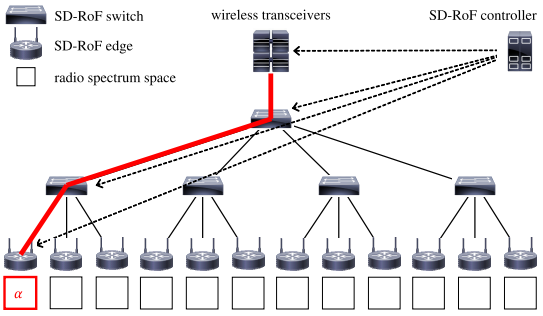


**FIGURE 3.** Elastic wireless service using SD-RoF.

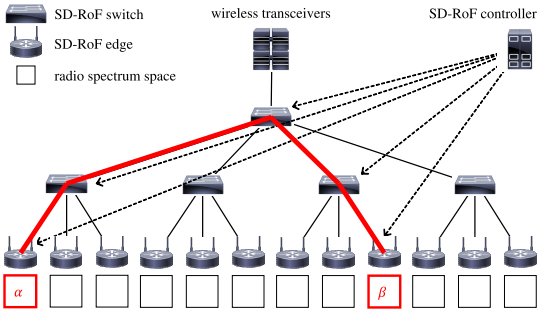


**FIGURE 4.** Elastic bidirectional passthrough using SD-RoF.

established by using an RoF analog band of just a few GHz. Moreover, it is possible to reduce transmission and processing delays, which is necessary for connecting to an IP network.

The subsequent sections of the manuscript are organized as follows. In Section II, the related works are described. In Section III, the components of SD-RoF are detailed. In Section IV, the performance analysis and experimental evaluation are discribed In Section V, the application scenarios, the deployment scenarios are discussed. In addition, the possibility of protocol optimization for SD-RoF is discussed. In Section VI, conclusion and future work are presented.

## II. RELATED WORKS

### A. SDN

SD-RoF was inspired by software-defined networks (SDNs). SDN constructs a virtual network by software control. In the legacy network, each communication device has its own OS, control software, route selection function, and data transfer function, so the network is fixed, and setting and configuration work for each device. The SDN separates a network into a control plane and a data plane and controls each device in the network from the controller, allowing flexible network setup and operation [2]. Examples of potential applications of SDN include network slicing [3], virtual private networks [4], and hybrid environments with conventional IP networks [5]. One of the advantages of building a virtual network is that the network configuration can be flexibly changed according to the use case. Since the low latency, high bandwidth, and reliability required by applications vary, optimization for specific use cases is required. On the other hand, the configurations for network optimization have some challenges. One of the challenges is the changing of network configuration. When changing the network configuration, it is desirable to maintain the reachability of packets without stopping the network. In response to this, research has been conducted to automatically generate procedures for updating to the desired network configuration and to verify configuration errors [6]. In addition, research is being conducted to minimize the frequency of network updates [7].

The difference between SD-RoF and SDN is that SDN mainly targets wired networks and achieves the setup and switching of networks at L2 or higher, whereas SD-RoF targets wireless access networks and establishes and switches them at L1. In SDN, each switch forward packets based on the forwarding rules aggregated in the controller. On the other hand, in SD-RoF, the controllers change the network configuration by switching the path in the optical switches.

### B. C-RAN

An example of an SDN-like approach being introduced to a wireless access network is the cloud radio access network (C-RAN). C-RAN is a generic term for a wireless access network that has separated base stations (BSs) and remote radio heads (RRHs). Various architectures that expand the concept of C-RAN to satisfy 5G application requirements have been proposed. Examples include FlexRAN [8], SoftAir [9], H-RAN [10], and F-RAN [11]. RoF-based C-RAN has been discussed as a high-capacity mobile fronthaul in 5G mobile networks [12], [13] However, it should be noted that most of the discussions on RoF-based C-RAN have mainly used D-RoF. Since the data rate required for 6G is more than 1 Tbps, D-RoF requires a very wide transmission bandwidth. To manage the rapidly increasing data rates, implementation costs will become a major challenge with D-RoF [14].

From this perspective, particularly, A-RoF-based C-RAN has attracted much attention in recent years [15], [16]. The analog-millimeter-wave-over-fiber fronthaul architecture [17] and the machine learning-based A-RoF C-RAN architecture [16] have also been discussed towards 6G communications. In these methods, the C-RAN is constructed by aggregating mobile signals using WDM. On the other hand, SD-RoF uses single-mode fiber as the transmission path and switches the transmission path at L1. Therefore, SD-RoF has advantages in terms of ease of control and costs. In addition, SD-RoF has novelty in the realization of architecture-based elastic bidirectional passthrough.

### C. EON

Elastic optical networks (EON) serve to exemplify technology that engenders greater flexibility in optical networks. EON can allocate optical path frequency resources to user requests in a detailed and flexible manner [18]. EON is achieved by multi-carrier high-order modulation and bandwidth wavelength selective switches. Various techniques to

improve the efficiency of optical frequency utilization in the network using EON were proposed. Examples includes EON with spatial division multiplexing (SDM) [19], integrate flexible Ethernet (FlexE) with EON [20], virtual network mapping in EON [21], and optimal multi-controller placement in inter-datacenter EON [22].

A notable difference between SD-RoF and EON is that, while elastic optical networks mainly focus on core networks and apply cutting-edge optical communication technologies, such as coherent optical receivers and optical OFDM, SD-RoF is focused on wireless access networks and employs legacy optical communication technology. SD-RoF is intended to work also on legacy optical networks.

## III. SD-RoF: SOFTWARE-DEFINED RADIO OVER FIBER

### A. ARCHITECTURE OVERVIEW

The proposed SD-RoF is a wireless access network designed to address the requirements of diversity, broadband capacity, and low latency. The radio spectrum space is therein defined as the space in which devices located in a certain area can directly communicate with each other. In a normal scenario, devices belonging to different radio spectrum spaces cannot directly communicate with each other. To address this limitation, SD-RoF is composed of an SD-RoF network built with an SD-RoF switch and an SD-RoF edge, an SD-RoF controller, wireless transceivers, and RoF. The SD-RoF controller switches the connection of the SD-RoF network.

### B. RoF

RoF is composed of two E/O converters connected by an optical fiber. RoF has traditionally been used for large capacity transmission from core to edge in mobile networks due to its high bandwidth and low latency. 6G mobile networks place high importance on RoF as a transmission path for high attenuation signals such as mmWave communications and terahertz communications [23].

There are two RoF types: analog and digital. The difference between analog RoF (A-RoF) and digital RoF (D-RoF) is based on whether the input/output to the RoF is an analog or digital signal. In analog RoF, an analog electric signal is directly converted to an optical signal, enabling broadband communication at a lower cost than with a digital RoF. For example, the transceivers of analog RoF that were used to implement a prototype of SD-RoF provided broadband transmission between 40 MHz and 6 GHz at a low cost, just a few hundred dollars. On one hand, however, analog RoF is susceptible to nonlinear distortion and noise generated in the optical transmitter. On the other hand, with digital RoF, the digital signals are transmitted by on-off keying of light. It is therefore not affected by nonlinear distortion and noise generated by the optical transmitter. Nevertheless, for its use in bidirectional communication in this study, it requires certain equipment, such as AD/DA converters and frequency converters, which increase the latency and cost. The proposed method uses analog RoF, resulting in its lower implementation cost and low latency.

### C. SD-RoF SWITCH

Figure 5 shows the configuration of an SD-RoF switch. It consists of an optical switch circuit, an elastic RoF module, and RoF transceivers. The function of an optical switch circuit is to switch the input and output of the optical signal according to the control command from the SD-RoF controller. The optical switch in SD-RoF is a simple one that switches the one-to-one relationship of input and output ports as a circuit. Because it does not involve packet processing, it can be accommodated with the same configuration regardless of the input signal format or data rate. An elastic RoF module has the function of frequency conversion and multiplexing of electric signals according to the control command from the SD-RoF controller. The wireless communication signal, which is converted into electricity by the RoF receiver, is frequency-converted and multiplexed. It is then converted back into an optical signal by the RoF transmitter. Accordingly, wireless communication signals that arrive from multiple paths are bundled as a single optical signal. This enables the optical frequency resource to be more efficient.

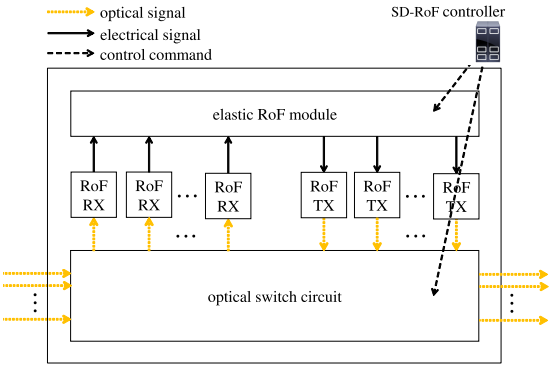


**FIGURE 5.** SD-RoF switch.

### D. SD-RoF EDGE

Figure 6 shows the configuration of an SD-RoF edge. SD-RoF is composed of an RoF transceiver, an elastic RoF module, an analog cancellator, and a transceiver antenna. The elastic RoF module has the same frequency conversion and multiplexing function as that used in the SD-RoF switch. For example, when performing MIMO transmission, it is necessary to deal with multiple signals of the same frequency

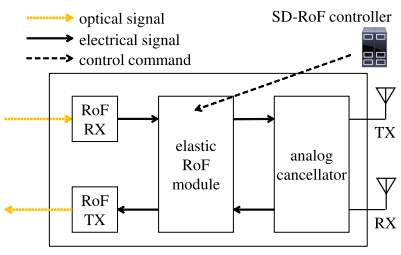


**FIGURE 6.** SD-RoF edge.

band with a single SD-RoF edge. Thus, by converting the signals of each channel into different frequencies, multiplexing them, and inputting them into RoF, it is possible to deliver them to the other SD-RoF edge as one optical signal. The role of an analog cancellator in this process, along with elastic bidirectional passthrough, is explained in Section III-F.

### E. ELASTIC RoF MODULE

The elastic RoF module provides frequency conversion and multiplexing of input signals in the SD-RoF edges and SD-RoF switches. The elastic RoF module acts as a passive signal path after the connection path is assured. Figure 7 shows the block diagram of the elastic RoF module. The elastic RoF module consists of a control command decoder, frequency converters, a switch matrix, and signal synthesizers.

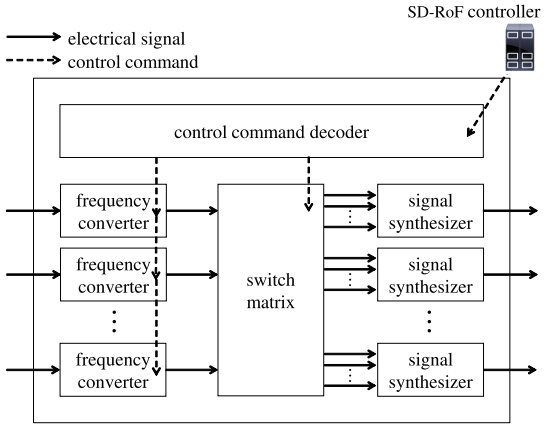


**FIGURE 7.** Elastic RoF module.

The control command decoder in the elastic RoF module receives a control command sent from the SD-RoF controller. The control command decoder interprets the control command and then configures each frequency converter and switch matrix. For the frequency converter, the control command decoder sets two carrier frequencies, $f_1$ before conversion and $f_2$ after conversion. For the switch matrix, the control commander sets the connection between the switch matrix input and the signal synthesizer input.

The signal inputted to the elastic SD-RoF module is first distributed. If frequency conversion is required, the output signal from the frequency converter is fed into the signal synthesizer. On the other hand, if frequency conversion is not required, the distributed signal, which does not pass through the frequency converter, is fed into the signal synthesizer. Figure 8 shows the structure of the frequency converter. The frequency setting and automatic gain control (AGC) circuit in Figure 8 automatically controls the gain of the low noise amplifier (LNA) and the voltage gain amplifier (VGA). This is done by acquiring the received signal strength indicator (RSSI) of the output signal from the VGA. The frequency converter is a function to avoid collisions with other communications by frequency-converting. The frequency converter

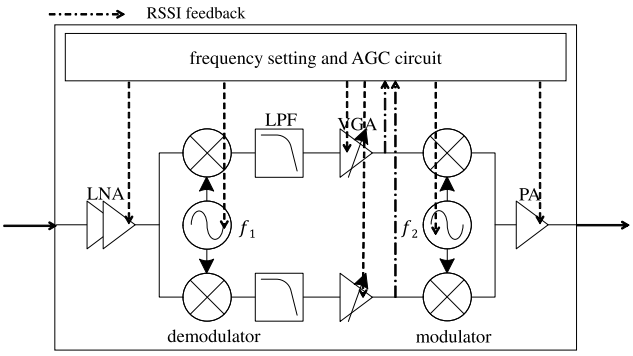


**FIGURE 8.** Frequency converter.

converts a signal transmitted at the carrier frequency $f_1$ to a signal transmitted at the carrier frequency $f_2$. The carrier frequencies $f_1$ and $f_2$ can be changed from the SD-RoF controller via the control command decoder and the frequency setting and AGC circuit, respectively. The frequency converter quadrature demodulates the input signal at the same frequency $f_1$ as the input signal and extracts the baseband signal with a low pass filter (LPF). The baseband signal is modulated with the carrier frequency $f_2$ to be frequency-converted. The frequency converter also performs as a filter circuit that extracts only the desired band.

The output signal from the frequency converter is fed into the switch matrix. The switch matrix allows an arbitrary switch matrix input to be matched to an arbitrary signal synthesizer input. The connections are switched electrically using RF switches.

The signal synthesizer superimposes multiple input signals and converts them into a single output signal. For example, in the case of the signal synthesizer that is capable of combining $n$ signals, inputting the signals $s_1(f_1)$, $s_2(f_2)$, $\cdots$, and $s_n(f_n)$ outputs the signal $s_1(f_1) + s_2(f_2) + \cdots + s_n(f_n)$. The signal of the center-frequency $f_k$ is defined as $s_k(f_k)$ $(k = 1, 2, \ldots, n)$, $s_k(f_k)$ is not over-wrapping for any $k$.

### F. ANALOG CANCELLATOR

In the proposed method, two SD-RoF edges are connected by two RoFs, one upstream and one downstream. When two SD-RoF edges are connected this way, two-way communication cannot be achieved by simply connecting two antennas. Figure 9 shows the signal loop problem that occurs when extending the wireless communication area with RoF. The signal sent from the terminal $\alpha$ is received by the receiver antenna of the SD-RoF edge $\alpha$ and transmitted from the transmit antenna of the SD-RoF edge $\beta$ via the RoF. Conversely, the signal sent from the terminal $\beta$ is received by the receiver antenna of the SD-RoF edge $\beta$ and transmitted from the transmit antenna of the SD-RoF edge $\alpha$ via the RoF. When a signal sent from the terminal $\alpha$ is transmitted by the transmit antenna of the SD-RoF edge $\beta$, the receiver antenna of the SD-RoF edge $\beta$ receives the signal as a self-interference signal. Moreover, the signal is transmitted from the transmit

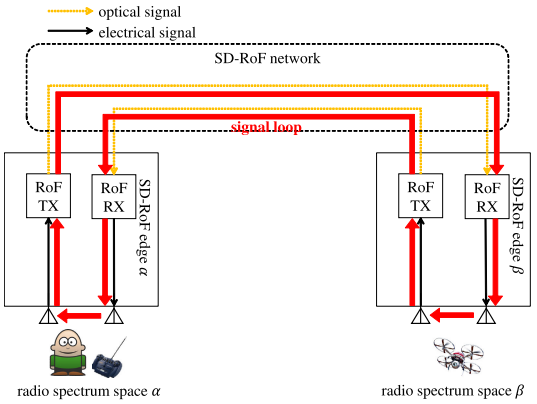


**FIGURE 9.** Radio signal loop between two SD-RoF edges.

antenna of the SD-RoF edge repeatedly, which occurs in an infinite loop and inhibits communication.

The proposed method uses an analog cancellator that combines a calibration circuit and an analog cancellator to solve the signal loop problem. Figure 10 shows the overview of the analog cancellation of the radio signal loop between two SD-RoF edges. In Figure 10, the loop signal shown in Figure 9 is canceled by equipping the SD-RoF edge with the analog cancellator shown in Figure 11. We used the passive cancellation circuit developed in [24] for full-duplex wireless communication as the analog cancellator.

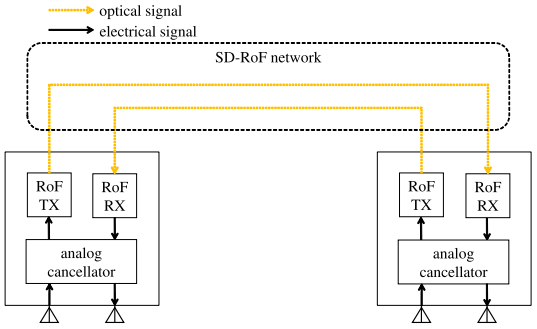


**FIGURE 10.** Analog cancellation of radio signal loop between two SD-RoF edges.

The structure of the analog cancellator shown in Figure 11 is described in detail. The analog cancellator shown in Figure 11 generates a signal with the antiphase and the same amplitude as the input signal. The looped signal is canceled by superimposing the generated antiphase signal with the signal received by the receiving antenna. The calibration circuit is shown in Figure 11 calibrates the passive elements of the analog cancellator. A transmitter in the calibration circuit sends out an unmodulated continuous wave and reproduces the multipath of the radio transmission path between the transmitter and receiver antennas. The parameters of the circuit are set passively by the micro-controller unit (MCU). The MCU receives the value of the power sensor included in the calibration circuit and sets the parameters to maximize the

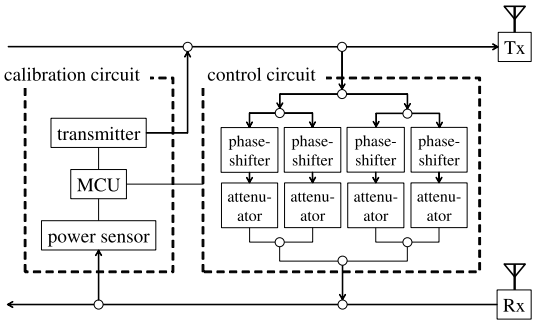


**FIGURE 11.** The configuration of analog cancellator.

cancellation amount. In environments where the surrounding environment significantly fluctuates (e.g., outdoor environments), it may be necessary to perform calibration periodically. The setting time for calibration is approximately 3.3 ms.

## IV. EVALUATION

### A. PERFORMANCE ANALYSIS

#### 1) SCALABILITY

To quantify the scalability with deploying elastic RoF modules, we evaluated the number of fiber optic cables between the SD-RoF networks. Figure 12 shows the SD-RoF network model for the evaluation. All radio spectrum spaces communicate over a wireless LAN with 2.412 GHz. When one SD-RoF edge is added to the SD-RoF switch 2 and one SD-RoF edge is added to the SD-RoF switch 3, a bidirectional communication path is established between the two SD-RoF edges. This path is defined as one interconnection. Each SD-RoF edge can use sixteen wavelengths. This number was chosen because the number of upstream/downstream wavelengths used in the NG-PON2 standard is limited to eight [25].

We compared the SD-RoF switch in three cases: 1) SD-RoF switch without the elastic RoF module, 2) SD-RoF switch with a wavelength selective switch (WSS) as an optical switch, but without the elastic RoF module, and 3) SD-RoF switch with the elastic RoF module. The WSS is an optical switch capable of multiplexing and demultiplexing optical signals in the optical domain. The WSS separates the input wavelength division multiplexing (WDM) signals for each wavelength and arbitrarily determines an output port for transmitting each separated signal. Figure 13 shows the number of fiber optic cables with 32 or fewer interconnections. The vertical axis represents the number of fiber optic cables between SD-RoF switch 1 and SD-RoF switch 2. In the case of 1) the SD-RoF switch without an elastic RoF module, the number of fiber optic cables increases linearly. Each interconnection uses a single fiber optic cable due to the SD-RoF switch is not capable of multiplexing. For 2) the SD-RoF switch with WSS as an optical switch, the number of fiber optic cables was increased for every 8 interconnections. The number of interconnections that can be accommodated by a single fiber optic cable is 8 due to each interconnection

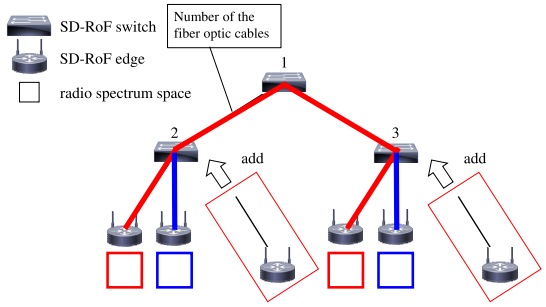


**FIGURE 12.** SD-RoF network evaluation model.

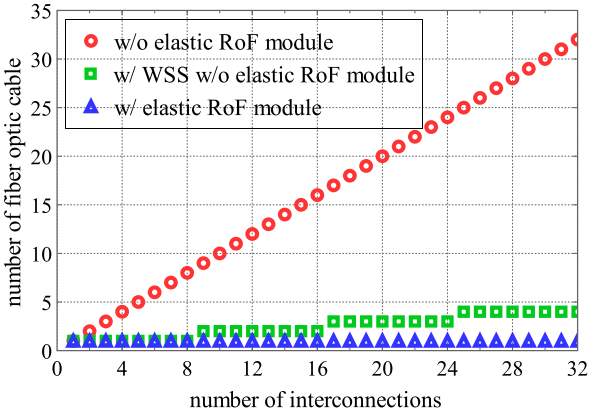


**FIGURE 13.** Number of fiber optic cables relative to the number of interconnections.

uses two wavelengths. For 3) the SD-RoF switch with the elastic RoF module, the number of fiber optic cables required was constant if the number of interconnections was below 32. This result shows that the addition of the elastic RoF module increases the flexibility and scalability of the SD-RoF network compared to those without the elastic RoF module.

The number of interconnections shared on a single fiber optic cable using the elastic RoF module is limited by the bandwidth supported by the RoF transceivers. The RoF transceiver supports several GHz transmissions. If an elastic RoF module multiplexes the signal from approximately 100 interconnections, using 50 MHz bandwidth for each interconnection, all interconnections consume 5 GHz for a single fiber optic cable. Therefore, we considered that all interconnections of fewer than 100 can be accommodated without additional fiber optic cables.

### 2) SIGNAL-TO-NOISE RATIO (SNR)

To describe qualitatively the effect of deploying an analog cancellator, we evaluated the SNR of elastic bidirectional passthrough. We considered $P_{tx}$ [dBm], which denotes the power of the signal transmitted from the terminal in base $\alpha$, $L_{rf}\ (d)$ [dB] denotes the attenuation when the distance in the wireless communication is d [m], $A_{rof}$ [dB] denotes the signal amplification rate of the RoF transmission module (RoF Tx), $nF_{rof}$ [dB] denotes the noise figure in the RoF, $L_{opt}\ (d)$ [dB] denotes the attenuation for optical communication over a distance d [m], $L_{ant}$ [dB] denotes the attenuation between the transmission and reception antennas in the SD-RoF edge, $C$ [dB] denotes the cancellation amount of the self-interference cancellation circuit, $S_n$ [dBm] denotes the power of the signal that reaches the transmission antenna point in the n-times loop, and $N$ [dBm] denotes the noise floor. $S_0$ is the strength of the initial signal that reaches the transmission antenna point in the SD-RoF edge $\beta$ from the SD-RoF edge $\alpha$. Subsequently, $S_0$ is determined as follows:

$$S_0 = P_{tx} - L_{rf}\ (d_\alpha) + A_{rof} - L_{opt}\left(d_{\alpha,\beta}\right) \tag{1}$$

$S_1$ denotes the strength of the initial signal that is returned to SD-RoF edge $\beta$. Subsequently, $S_1$ is determined as follows:

$$S_1 = S_0 - 2\Lambda\left(d_{\alpha,\beta}\right)$$

Furthermore, $\Lambda\ (d)$ is the attenuation for distance $d$ [m] between the SD-RoF edges.

$$\Lambda\ (d) = L_{ant} + C - A_{rof} + L_{opt}\ (d) \tag{2}$$

Moreover, if $S_n$ denotes the strength of the signal that loops $n$-times, then $S_n$ is generally determined as follows:

$$S_n = S_{n-1} - 2\Lambda\left(d_{\alpha,\beta}\right) \quad \text{if } n > 0$$

Furthermore, if $N_{\beta,ant}$ denotes the initial noise-signal strength attained at the transmission antenna of base $\beta$ from base $\alpha$; then $N_{\beta,ant}$ is determined as follows:

$$N_{\beta,ant} = \max\left(N + A_{rof} + nF_{rof}, \Sigma_{i=1}^{\infty} S_i\right)$$

If $\Lambda\left(d_{\alpha,\beta}\right) \leq 0$, then it is impossible to communicate because the self-interference wave continues to amplify. Therefore, assuming $\Lambda\left(d_{\alpha,\beta}\right) > 0$, the following equation is satisfied.

$$S_{n+1} < S_n \quad \text{if } n \geq 0$$

Furthermore, assuming that $S_{n+1} \ll S_n$, $N_{\beta,ant}$ is determined by the following equation:

$$N_{\beta,ant} = \max\left(N + A_{rof} + nF_{rof}, S_1\right) \tag{3}$$

Hence, from equation (1) and equation (3), $SNR_\beta$ is determined using the following equation:

$$SNR_\beta = S_0 - L_{rf}\left(d_\beta\right) - \max\left(N, N_{\beta,ant} - L_{rf}\left(d_\beta\right)\right) \tag{4}$$

### 3) ROUND-TRIP-TIME (RTT)

To describe qualitatively the latency, we evaluated RTT of elastic bidirectional passthrough. We considered $D$ [bytes] as the size of transmitted packets, $B_{radio}$ [bps] as the communication speed of the terminal, and $c_{rof}$ [m/s] as the propagation speed in the optical fibers. In the proposed method, latency denotes the total time of propagation delay of the optical fiber ($T_{fiber}$), transmission delay in the wireless section ($T_{radio}$), processing delay ($T_{proc}$), and congestion delay ($T_{con}$). Incidentally, the transmission delay is absent in the wired section because the RoF is used for analog transmission. In the analysis, we ignore the time to pass through wireless communication and electronic circuits. Here, $T_{proc}$ corresponds to a

constant because it is generally smaller than the propagation and transmission delays, and $T_{con}$ is a constant because it is a temporary factor based on the status of the transmission line.

If $T_{fiber}$ denotes the time taken for a data packet to pass through $d_{\alpha,\beta}$ from terminal $\alpha$ to terminal $\beta$, then $T_{fiber}$ is determined by the following equation:

$$T_{fiber} = \frac{d_{\alpha,\beta}}{c_{fiber}} \tag{5}$$

In addition, $T_{radio}$ is determined by the following equation.

$$T_{radio} = \frac{8D}{B_{radio}} \tag{6}$$

Therefore, $T_{delay,proposed}$ denotes the time required for data to travel from terminal $\alpha$ to $\beta$ via the proposed method. Hence, $T_{delay,proposed}$ is determined by the following equation:

$$T_{delay,proposed} = T_{fiber} + 2T_{radio} + T_{proc} + T_{con} \tag{7}$$

Hence, if $T_{rtt,proposed}$ denotes the RTT taken to communicate between terminals $\alpha$ and $\beta$ via proposed method, $T_{rtt,proposed}$ can be determined by the following equation:

$$\begin{aligned} T_{rtt,proposed} &= 2T_{delay,proposed} \\ &= \frac{2d_{\alpha,\beta}}{c_{fiber}} + \frac{32D}{B_{radio}} + 2T_{proc} + 2T_{con} \end{aligned} \tag{8}$$

### B. COST ESTIMATION BY PROTOTYPE IMPLEMENTATION

#### 1) ELASTIC RoF MODULE

We implemented an elastic RoF module with four frequency converters, one switch matrix, and four signal synthesizers. Table 1 shows the parts used in the implemented elastic RoF module. The total cost of the parts was approximately $995. In the frequency converter, the frequency setting and AGC circuit used one STMicroelectronics STM32F446, four Texas Instruments TLV3201, and four Linear Technology LTC2630. In addition, the LNA, demodulator, LPF, and VGA used one Maxim Integrated MAX2830ETM [26] and the modulator and PA used one Maxim Integrated MAX2830ETM. The control command decoder used one STMicroelectronics STM32F446. The switch matrix was composed of one Anaren PD2328J5050S2HFs and forty-eight Panasonic Electric Works ARS1412s [27]. The signal synthesizer used one Anaren PD2328J5050S2HF. This implementation result shows that inexpensive devices can be used to construct flexible SD-RoF networks compared to devices used in elastic optical networks and recent core networks.

#### 2) ANALOG CANCELLATOR

We implemented an analog cancellator with four attenuators, four phase-shifters, one transmitter, and one controller. Table 2 shows the parts used in the implemented elastic RoF module. The total cost of the parts was approximately $351.53. The analog cancellator was composed of Skyworks SKY12343-364LF as the attenuator and M/A-COM Technology Solutions Inc. MAPS-010164 as the phase shifter.

**TABLE 1. Parts of elastic RoF module.**

| parts | unit cost [$] | quantity | cost [$] |
|---|---|---|---|
| STM32F446RET6 | 8.45 | 5 | 42.25 |
| MAX2830ETM | 9.26 | 8 | 74.08 |
| TLV3201AIDBVR | 1.20 | 16 | 19.20 |
| LTC2630CSC6-HZ10 | 3.53 | 16 | 56.48 |
| ARS1412 | 6.77 | 48 | 324.96 |
| PD2328J5050S2HF | 0.75 | 8 | 6.00 |
| other parts | – | – | 471.73 |
| total | | | 994.70 |

**TABLE 2. Parts of analog cancellator.**

| parts | unit cost [$] | quantity | cost [$] |
|---|---|---|---|
| SKY12343-364LF | 6.89 | 4 | 27.56 |
| MAPS-010164 | 71.41 | 4 | 285.64 |
| CC2531F128 | 8.09 | 1 | 8.09 |
| C8051F360 | 11.89 | 1 | 11.89 |
| other parts | – | – | 18.35 |
| total | | | 351.53 |

The transmitting circuit for calibration was composed of Texas Instruments CC2531F128 and Silicon Labs C8051F360.

### C. EXPERIMENTAL EVALUATION BY PROTOTYPE IMPLEMENTATION

#### 1) ELASTIC RoF MODULE

Table 3(a), (b) show basic characteristics of the elastic RoF module. The noise figure of the frequency converter was approximately 15 dB. The frequency switching delay of the frequency converter was typically 30 $\mu s$ due to the frequency reset time of the MAX2830ETM. The insertion loss of the switch matrix and signal synthesizer was approximately 10.4 dB, and the average isolation was approximately 48.6 dB for each input/output port. The insertion loss included the distribution loss of signals in the signal synthesizers and the switch matrix. Average isolation means that the undesired input signal is added to the output signal as 48.6 dB lower

**TABLE 3. Basic characteristics of elastic RoF module.**

(a) Frequency converter

| Characteristics | Value |
|---|---|
| Noise figure [dB] | 15 |
| Frequency switching delay [$\mu$s] | typ. 30 |

(b) Switch matrix and signal synthesizer

| Characteristics | Value |
|---|---|
| Insertion loss [dB] | 10.4 |
| Average isolation[dB] | 48.6 |
| Switching delay [ms] | max. 10 |

power noise. The switching delay for the switch matrix configuration change is expected to be within 10 ms due to the switching time of the Panasonic Electric Works ARS1412.

Figure 14 shows that experiment environment. Each signal transmitter generated the 2.412 GHz OFDM signal of 20 MHz bandwidth. The elastic RoF module received these signals, performed frequency conversion to one of them, and multiplexing them. The output signal of the elastic RoF module was fed into the spectrum analyzer.

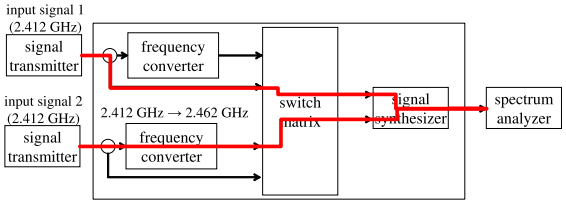


**FIGURE 14.** Experiment environment of elastic RoF module.

Figure 15 shows the results of frequency conversion and multiplexing using the elastic RoF module. Figure 15(a), (b) shows two 2.412 GHz OFDM signal waveforms as input to the elastic RoF module. The input signal 1 shown in Figure 15(a) was not frequency-converted. The input signal 2 shown in Figure 15(b) was frequency-converted to 2.462 GHz. Figure 15(c) shows the signal waveform of the output signal from the elastic RoF module. From Figure 15(c), it was confirmed that input signal 1 without frequency conversion and input signal 2 with frequency conversion from 2.412 GHz to 2.462 GHz were multiplexed. The signal synthesizer and switch matrix reduced the power of the input signal 1 and the input signal 2. This result shows that the implemented elastic RoF module has the functions required to share a single fiber optic cable with multiple SD-RoF edges. However, the input signal 2 was increased bandwidth than the original signal due to the noise of the frequency converter. It is necessary to properly determine the conversion frequency to avoid interference of the electrical signals in multiplexing due to the increased occupied bandwidth after the frequency conversion.

### 2) ANALOG CANCELLATOR

To confirm the cancellation performance of the analog cancellator that constitutes the proposed method, we measured the received signal strength indication (RSSI) of the signal before and after self-interference cancellation using a spectrum analyzer. Specifically, we measured the cancellation performance for unmodulated continuous waves and the cancellation performance for IEEE 802.15.4 data packets.

Figure 16 shows the evaluation environment for the self-interference cancellation performance of the analog cancellator. The transmitted signal was distributed as input to the analog cancellator and the attenuator. The attenuator simulated the propagation path between the transmitting and receiving antennas of the same SD-RoF edge, and the attenuation value corresponding to 10 dB. The self-interference

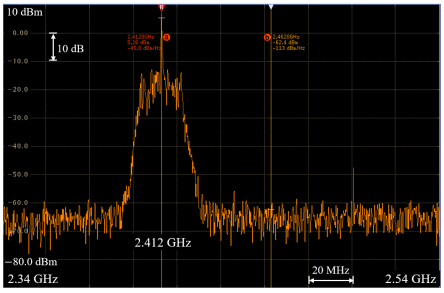


**(a)** Input OFDM signal 1

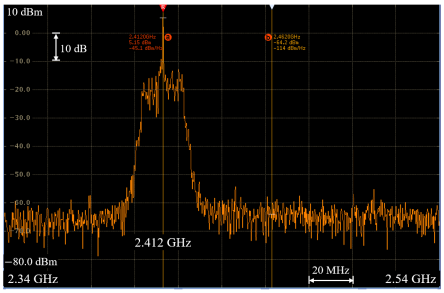


**(b)** Input OFDM signal 2 (before frequency-converting from 2.412 GHz to 2.462 GHz)

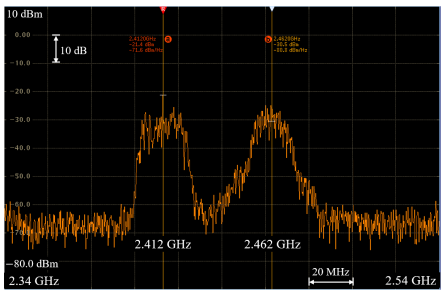


**(c)** Output signal

**FIGURE 15.** Frequency conversion and multiplexing of OFDM signals using elastic RoF Module.

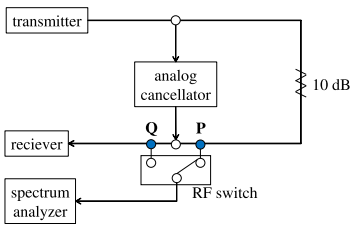


**FIGURE 16.** Evaluation environment for the self-interference cancellation performance of the analog cancellator.

signal was reproduced by the signal through the attenuator. After calibrating with a signal corresponding to the center frequency of 2,440 MHz, the experiment was performed by changing the frequency of the unmodulated continuous wave input from the transmitter in the range 2,400 to 2,480 MHz. The amplification factor $A_{rof}$ of RoF is 3 dB. The RSSI was measured at points P and Q as shown in Figure 16. The RSSI of the signal before self-interference cancellation is measured at point P, and the RSSI of the signal after self-interference

cancellation is measured at point Q. The cancellation amount was determined by comparing RSSI at points P and Q.

Figure 17 shows the cancellation amount for the unmodulated continuous wave with a center frequency of 2, 400 to 2, 480 MHz and the cancellation amount for the IEEE 802.15.4 data packets with a center frequency of 2, 400 to 2, 480 MHz. The horizontal axis denotes the frequency of the input signal, and the vertical axis denotes the cancellation amount. Figure 17 shows that up to approximately 54 dB self-interference cancellation is achieved for unmodulated continuous waves. Conversely, up to approximately 45 dB self-interference cancellation is achieved for IEEE 802.15.4 data packets. Because the bandwidth of IEEE 802.15.4 is 2 MHz, the cancellation performance is considered to be reduced compared to the unmodulated continuous wave.

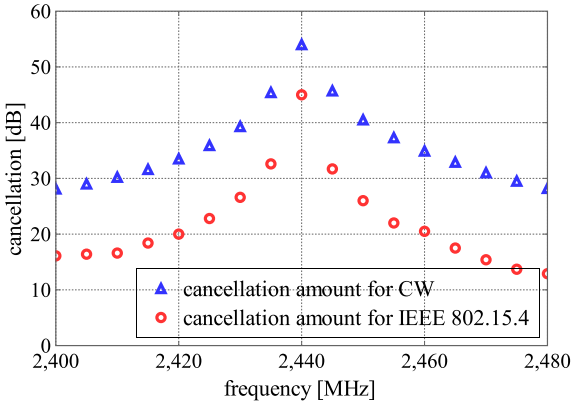


**FIGURE 17.** Measured cancellation performance of analog cancellator.

### D. DEMONSTRATION OF ELASTIC BIDIRECTIONAL PASSTHROUGH

We evaluated elastic bidirectional passthrough in three ways: packet error rate (PER), RTT and protocol applicability.

In PER and RTT evaluation, the transmitting circuit was composed of CC2531F128. CC2531F128 is a wireless transmission/reception module that includes the function of transmitting unmodulated continuous waves and the function of transmitting IEEE 802.15.4 data packets. The transmission frequency corresponded to 2,440 MHz and the transmission power corresponded to 0 dBm. The SD-RoF edge was composed of the transmission antenna, reception antenna, and analog cancellator. The RoF transmitter and receiver used ET-615 and ER-615, respectively. The operation was performed via the FTDI Virtual COM Port Driver. Terminals $\alpha$ and $\beta$ were placed in the shield box and shield tent to prevent direct wireless communication between terminals $\alpha$ and $\beta$, respectively. The shield box used a shield-cube of 45 cm (450 × 450 × 450 [mm]) made by TOYO Corporation. The shielding performance approximately corresponded to 60 dB measured. The shield tent used the EMI shield tent (2400 × 4800 × 2000 [mm]) made by TEIESJAPAN Corporation. The shielding performance approximately corresponded to 50 dB measured.

#### 1) PER

To evaluate the communication feasibility of a wireless access network, we measured the PER. Specifically, we measured the PER of packet transmission from terminal $\alpha$ to terminal $\beta$ while changing the amplification values in the RoF ($A_{rof}$) and compared it with and without the amplitude and insertion of the delay control circuit. To increase the communication distance of each SD-RoF edge, it is desirable to set a large value of $A_{rof}$.

Figure 18 shows the evaluation environment with the analog cancellator, and Figure 19 shows the evaluation environment without the analog cancellator. The evaluation was executed with the terminals and SD-RoF edges connected to a coaxial cable. To reproduce the self-interference between the transmitting and receiving antennas at each base station, we inserted attenuators between the transmitting and receiving antennas of the SD-RoF edges. The attenuation between antennas was approximately 10 dB. Furthermore, the transmitter of the terminals and receiving antennas of SD-RoF edges were connected using an attenuator to reproduce the propagation loss between the terminals and SD-RoF edges. The propagation loss between the terminals and SD-RoF edges was approximately 40 dB. The SD-RoF edges were connected to optical fibers with a length of 20 km.

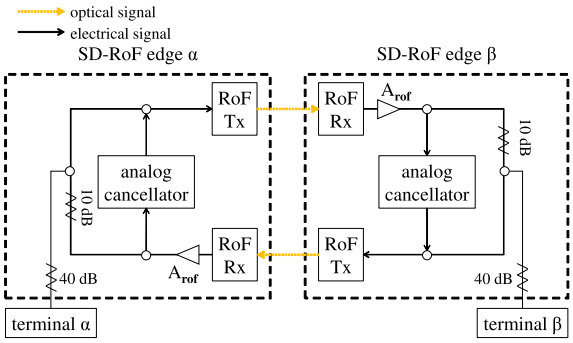


**FIGURE 18.** Evaluation environment with analog cancellator.

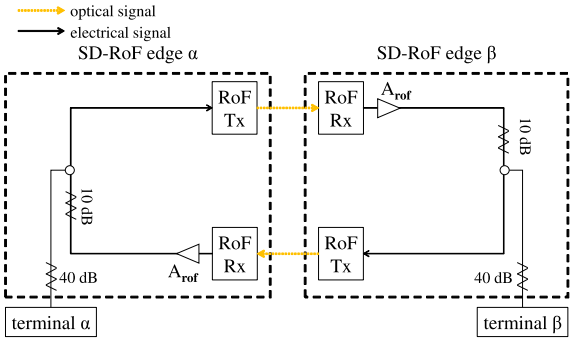


**FIGURE 19.** Evaluation environment without analog cancellator.

In the evaluation, $P_{tx}$ [dBm] is 0 dBm, $L_{rf}(d_\alpha)$ [dB] and $L_{rf}(d_\beta)$ [dB] are 43 dB, $NF_{rof}$ [dB] is 17 dB, $d_{\alpha,\beta}$ [km] is 20 km, $L_{opt}(d_{\alpha,\beta})$ [dB] is 4 dB, $L_{ant}$ [dB] is 15 dB, and $N$ [dB] is $-97$ dB. Incidentally, we assumed that the attenuation in the optical fiber is 0.2 dB/km. Furthermore, for the values $L_{rf}(d_\alpha)$ [dB], $L_{rf}(d_\beta)$ and $L_{ant}$ [dB], we considered the attenuation at the splitter. From equation (4), $SNR_\beta$ in this evaluation environment is determined by the following equation.

$$SNR_\beta = \begin{cases} A_{rof} + 7 & \text{if } A_{rof} < \frac{31+2C}{3} \\ 38 + 2C - 2A_{rof} & \text{else} \end{cases} \tag{9}$$

The required SNR in IEEE 802.15.4 is 5 dB or more. Further, $C$ [dB] is 0 dB without the analog cancellator. Hence, from equation (9), the conditions in which communication is possible are determined as follows.

$$-2 \leq A_{rof} \leq 16.5 \quad \text{if } C = 0, \tag{10}$$

Conversely, $C$ [dB] is 45 dB with an analog cancellator. Hence, from equation (9), the conditions in which communication is possible are determined as follows.

$$1 \leq A_{rof} \leq 61.5 \quad \text{if } C = 45 \tag{11}$$

From Equations 10 and 11, communication is possible only when the analog cancellator is used, when $16.5 < A_{rof} \leq 61.5$.

Figure 20 shows the comparison of PER with and without the analog cancellator. The measured results in Figure 20 show that the case without an analog cancellator has a lower PER and a higher communication quality when $A_{rof}$ is less than 8 dB. The insertion of an analog cancellator results in attenuation of the signal by the splitter and causes packet errors. Conversely, the communication quality with the circuit exceeded the one without the circuit when the amplification value at the RoF was 12 dB or more. By inserting the analog cancellator, it is possible to cancel the self-interfering signals owing to the increase in amplification at the RoF and communication.

The measured results in Figure 20 show that the results are close to the theoretical analysis. Conversely, in both cases, the communication availability condition is narrower in the measured result in Figure 20 compared to the theoretical result in Figure 20. This may be owing to the nonlinear distortion and noise susceptibility of analog RoFs.

### 2) RTT

To confirm the latency characteristics of the proposed method, we measured the RTT. Figure 18 shows the evaluation environment of the RTT in the proposed method. In this experiment, the RTT represented the time from when the terminal $\alpha$ started transmitting an IEEE 802.15.4 data packet to when terminal $\alpha$ finished receiving the acknowledgment (ACK) packets from terminal $\beta$. Terminals and SD-RoF edges were connected wirelessly. Terminal $\alpha$ sends IEEE 802.15.4 data packets to the terminal $\beta$, and terminal $\beta$ that receives the data packets sends ACK packets to the terminal $\alpha$. The size of the data packets was corresponding to 44 bytes, and the size of the ACK packets corresponding to 24 bytes. Terminal $\alpha$ retransmitted if ACK packets from terminal $\beta$ could not be received within 1 ms. The maximum number of carrier sense multiple access with collision avoidance (CSMA/CA) and retransmissions were 5 times and 3 times the recommended values of IEEE 802.15.4, respectively. The time was measured with the 16-bit timer of 1.6 MHz in CC2531F128.

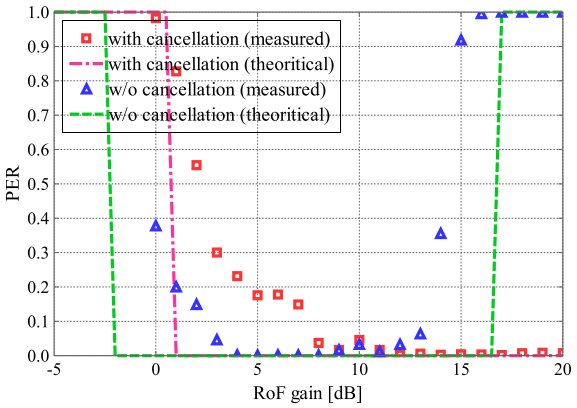


**FIGURE 20.** Comparison of PER with and without the analog cancellator.

Figure 21 shows the comparison of the measured RTT and theoretical RTT derived from equation (8). The measured RTTs were approximately 1,120 $\mu$s, 1,140 $\mu$s, 1,160 $\mu$s, 1,110 $\mu$s, 1,310 $\mu$s, 1,410 $\mu$s, and 1,510 $\mu$s for the lengths of 1 km, 3 km, 5 km, 10 km, 20 km, 30 km, and 40 km, respectively. In the calculation of the theoretical values, we considered the light speed in the optical fiber $c_{rof}$, which was approximately $2.053 \times 10^8$ [m/s], $B_{radio}$ was 250 kbps, and $D$ was 17 bytes. Incidentally, the light speed in the optical fiber $c_{rof}$ was determined by the light speed ($c = 2.998 \times 10^8$ [m/s]) and refractive index of the optical fiber ($n = 1.46$). As shown in Figure 21, a correlation

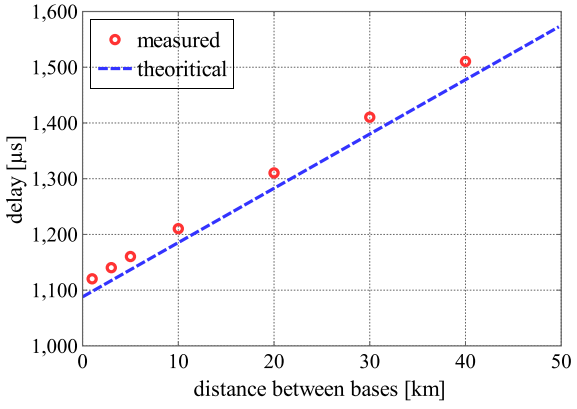


**FIGURE 21.** Comparison of the measured RTT and theoretical RTT derived from equation (8).

**TABLE 4.** The protocol applicability for SD-RoF.

| | 1 m | 200 m | 600 m | 1000 m | 3000 m | 5000 m | 10000 m | 20000 m |
|---|---|---|---|---|---|---|---|---|
| IEEE 802.15.4 | ✓ | ✓ | ✓ | ✓ | ✓ | ✓ | ✓ | ✓ |
| IEEE 802.11bg | ✓ | ✓ | ✓ | ✓ | ✓ | | | |
| BR/EDR | ✓ | ✓ | ✓ | ✓ | | | | |
| BLE | ✓ | ✓ | ✓ | ✓ | | | | |

exists between the measured and theoretical results. It was confirmed that the proposed method achieved low latency communication of less than 1 ms in one direction for the length of 40 km.

#### 3) PROTOCOL APPLICABILITY

To evaluate the applicability of existing communication protocols to SD-RoF, we investigated the possibility of communication for several communication protocols. More specifically, we conducted experiments by changing the optical fiber length of each communication protocol to clarify the range in which direct communication through SD-RoF is possible. We used IEEE 802.11bg, IEEE 802.15.4, Bluetooth BR/EDR, and Bluetooth BLE, which are communication protocols in the 2.4GHz band, for the experiments. The lengths of the optical fibers used were 1 m, 200 m, 600 m, 1,000 m, 3,000 m, 5,000 m, 10,000 m, and 20,000 m. The terminal used in Section IV-D was used as the IEEE 802.15.4 communication terminal. As communication terminals for IEEE 802.11bg, we used Buffalo's WZR-300HP and WZR-600DHP. We used two PCs as Bluetooth BR/EDR communication terminals to transfer files between PCs. We confirmed the connection of a smartphone and a smartwatch as Bluetooth BLE communication terminals.

The results are shown in Table 4. IEEE 802.15.4 is able to communicate for all distances used in this experiment. However, at 20,000 m, retransmissions always occurred. At longer distances, the ACK timeout, number of retransmissions, and collisions are likely to prevent communication.

On the other hand, IEEE 802.11bg can only communicate up to 3,000 m. It is thought that the CSMA/CA does not work properly due to the long-distance transmission, and communication is not possible.

As for BR/EDR and BLE, they can only communicate up to 1,000 m. This is thought to be since the time synchronization protocol of Bluetooth cannot support long-distance transmission. More specifically, the time synchronization gap between master and slave that can be tolerated by Bluetooth is $\pm 10\ \mu$s. Since optical fiber transmission has a propagation delay of 5 $\mu$s per 1 km, a round-trip propagation delay of 10 $\mu$s occurs when connecting locations with 1,000 m optical fibers. Therefore, it is considered that Bluetooth cannot communicate in the range of 3,000 m or more.

## V. DISCUSSION

### A. APPLICATION SCENARIOS

#### 1) SOFTWARE-DEFINED WiFi

Software-Defined WiFi (SD-WiFi) enables the user to leverage a WiFi connection that supports the desired functions according to the user's location. It is built with an elastic wireless service function, as shown in Figure 3. With SD-WiFi, the user can remotely update the WiFi to a new standard without physically replacing the WiFi access point. The user can even employ their own WiFi access point when they are in a remote location. Even if only 2.4 GHz and 5 GHz bands are the research focus, the WiFi standards continue to be updated from one protocol to another, as demonstrated with IEEE 802.11b, IEEE 802.11a, IEEE 802.11g, IEEE 802.11n, and IEEE 802.11ac. In some cases, with commercial WiFi, different transmission speeds are evident, even when they are claimed to operate under the same standards. With the introduction of SD-WiFi, however, the user can easily add new functionality to their WiFi via a simple browser setting. Accordingly, the user can employ, for example, an inexpensive IEEE 802.11g, for regular domestic use and temporarily upgrade it to high-speed IEEE 802.11ac to view a 4K high-definition film.

Furthermore, when a user connects to the Internet when away from home, the current standard procedure is to connect to a public wireless LAN provided in commercial establishments and public transport. However, these connections are vulnerable to security breaches, such as unauthorized access, interceptions, and virus infections. With the implementation of SD-WiFi, the user can employ their personal WiFi access point at any time and place.

#### 2) REMOTE MANIPULATION

Remote manipulation means controlling vehicles, heavy machinery, and robots via a network. In this approach, dangerous tasks, such as dismantling buildings, can be executed, and robots can perform surgeries remotely. These are some potential applications of the elastic bidirectional passthrough depicted in Figure 4. In remote manipulation scenarios, the operator controls the equipment based on the video captured from a connected camera. This type of procedure requires low latency with broadband communication capabilities in transmitting the video and low latency with highly reliable communication capabilities when sending the operational signals. However, with current wireless access networks, executing a remote manipulation at the same level as a direct operation is difficult owing to video codec and communication latencies. The communication provided by SD-RoF, on the other hand, works as if an uncompressed video is being directly sent from the camera to the display. This reduces the delays to near-zero levels. Furthermore, since it is possible to configure a flexible network with SD-RoF, centralized remote-operation rooms could be

established for various unexpected emergencies. Such rooms could enable a more rapid response to local disasters, whereby remotely manipulated, unmanned rescue operations could be more efficiently conducted.

#### 3) ESPORTS

A potential application of SD-WiFi is esports, specifically online game matches using remote peer-to-peer (P2P) communication among multiple users located in different radio spectrum spaces. The remote operations discussed in Section V-A3 are based on elastic bidirectional passthrough between two points, as shown in Figure 4. However, in this section, the elastic bidirectional passthrough involves three or more points. In highly competitive esports games, such as fighting games, first-person shooting (FPS), and third-person shooting (TPS), lag can have a major impact on the outcome. For this reason, the competitors often still prefer to take their computers and compatible home video game consoles to a physical location, rather than playing online. With SD-RoF, the competitors can play games against one another as if they are sharing the same space even from a distance because their wireless signals are directly exchanged with low latencies.

### B. DEPLOYMENT SCENARIO

This section discusses the introduction of SD-RoF into FTTH, a wired access network consisting entirely of optical fiber from the base station to the user's house [28]. Some of the advantages of fiber-optic communication a high transmission speed and stability. Given the need to implement networks that offer both a large capacity and low latency, the FTTH adoption rate is expected to increase significantly in the coming years.

Currently, the most commonly used system that enables FTTH is a passive optical network (PON). Figure 22 shows the configuration of a PON. It is composed of an optical line terminal (OLT), an optical distribution network (ODN), and an optical network terminal (ONT). An OLT is a function that mutually converts electrical and optical signals on the network side. An ODN is a function that distributes optical signals from the OLT to multiple ONTs, aggregates the signals of multiple ONTs, and transmits them to the OLT. An ONT is a function that mutually converts optical and electrical signals at the user's house. The user establishes a LAN under the ONT to access the network. G-PON recommendation regulates the maximum fiber distance between OLTs and ONTs of up to 60 km and the split ratios of up to 1:64 as the requirements for the physical layer [29].

Figure 22 shows the deployment of SD-RoF to the FTTH. By replacing the OLT on a PON with a wireless transceiver, the ODN with an SD-RoF switch, and the ONT with an SD-RoF edge, it is possible to provide SD-RoF. If SD-RoF is introduced and elastic bidirectional passthrough is used, multiple devices can communicate with each other without having to return the core network.

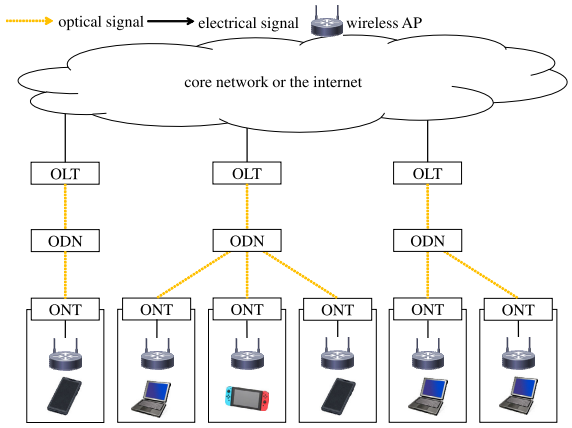


**FIGURE 22.** FTTH using PON.

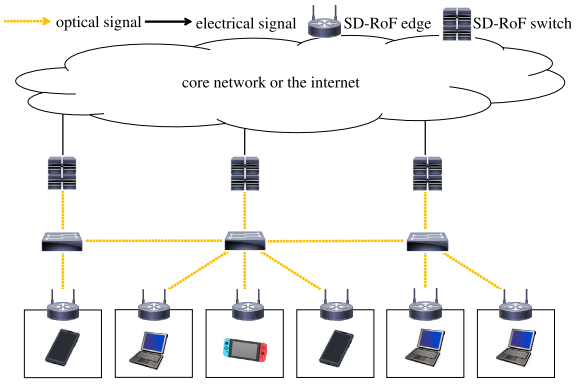


**FIGURE 23.** SD-RoF deployment example.

### C. PROTOCOL OPTIMIZATION

In [30], it is proposed that CSMA/CA can work properly by extending the slot time. The slot time defined in IEEE 802.11 standard [31] is 9 [$\mu$s]. In SD-RoF, it is necessary to consider the propagation delay of the optical fiber. If the propagation delay due to the optical fiber is 5$\mu$ [s/km], it can be determined as follows when the length of the optical fiber is $a$ [km]. The propagation delay by the optical fiber is approximately 5$\mu$ [s/km]. Therefore, if the length of the optical fiber is $a$ [km], the slot time must be $9 + 2a$ [$\mu$s]. The space propagation delay is defined in the IEEE 802.15.4 standard, and the maximum space propagation delay can be set to 114,750 m. By setting a large class, it is possible to realize communication via SD-RoF without changing the existing protocol in any optical fiber length.

However, extending slot time increases the backoff time. The longer the backoff time, the fewer opportunities there are to transmit packets. Therefore, this method suffers from a sharp drop in throughput during long-distance communication. In contrast, [32] proposes to operate CSMA/CA normally by adjusting the network allocation vector (NAV) period. Compared to the method of changing the slot time, adjusting the NAV period can reduce the throughput degradation. To set optimal parameters or to develop new optimal protocols is necessary to improve the applicability.

## VI. CONCLUSION

We proposed SD-RoF, an architecture that tightly couples optical and radio technologies. The two functions that are required to achieve this objective are the elastic wireless service and elastic bidirectional passthrough. In this paper, we design and prototype implementation of SD-RoF, and conduct a basic evaluation of the implemented circuit and demonstration experiments on elastic bidirectional passthrough. The results show that devices using short-range wireless communication protocols such as IEEE 802.15.4 and IEEE 802.11 can communicate with each other over a distance of several kilometers via SD-RoF. However, the distance that can be communicated via SD-RoF differs for each protocol due to the propagation delay on fiber. It is necessary to communicate within the acceptable area or to extend the communication distance by optimizing parameters to use the existing protocols on SD-RoF.

## REFERENCES

[1] Q. Zhang, J. Liu, and G. Zhao, "Towards 5G enabled tactile robotic telesurgery," 2018, *arXiv:1803.03586*. [Online]. Available: http://arxiv.org/abs/1803.03586

[2] J. H. Cox, J. Chung, S. Donovan, J. Ivey, R. J. Clark, G. Riley, and H. L. Owen, "Advancing software-defined networks: A survey," *IEEE Access*, vol. 5, pp. 25487–25526, 2017.

[3] J. Ordonez-Lucena, P. Ameigeiras, D. Lopez, J. J. Ramos-Munoz, J. Lorca, and J. Folgueira, "Network slicing for 5G with SDN/NFV: Concepts, architectures, and challenges," *IEEE Commun. Mag.*, vol. 55, no. 5, pp. 80–87, May 2017.

[4] K. A. Noghani, C. H. Benet, A. Kassler, A. Marotta, P. Jestin, and V. V. Srivastava, "Automating Ethernet VPN deployment in SDN-based data centers," in *Proc. 4th Int. Conf. Softw. Defined Syst. (SDS)*, May 2017, pp. 61–66.

[5] D. K. Hong, Y. Ma, S. Banerjee, and Z. M. Mao, "Incremental deployment of SDN in hybrid enterprise and ISP networks," in *Proc. Symp. SDN Res.*, Mar. 2016, pp. 1–7.

[6] M. Reitblatt, N. Foster, J. Rexford, C. Schlesinger, and D. Walker, "Abstractions for network update," in *Proc. ACM SIGCOMM Conf. Appl., Technol., Archit., Protocols Comput. Commun. (SIGCOMM)*, 2012, p. 323.

[7] A. Destounis, S. Paris, L. Maggi, G. S. Paschos, and J. Leguay, "Minimum cost SDN routing with reconfiguration frequency constraints," *IEEE/ACM Trans. Netw.*, vol. 26, no. 4, pp. 1577–1590, Aug. 2018.

[8] X. Foukas, N. Nikaein, M. M. Kassem, M. K. Marina, and K. Kontovasilis, "FlexRAN: A flexible and programmable platform for software-defined radio access networks," in *Proc. 12th Int. Conf. Emerg. Netw. Exp. Technol.*, Dec. 2016, pp. 427–441.

[9] I. F. Akyildiz, P. Wang, and S.-C. Lin, "SoftAir: A software defined networking architecture for 5G wireless systems," *Comput. Netw.*, vol. 85, pp. 1–18, Jul. 2015.

[10] M. Peng, Y. Li, J. Jiang, J. Li, and C. Wang, "Heterogeneous cloud radio access networks: A new perspective for enhancing spectral and energy efficiencies," *IEEE Wireless Commun.*, vol. 21, no. 6, pp. 126–135, Dec. 2014.

[11] M. Peng, S. Yan, K. Zhang, and C. Wang, "Fog-computing-based radio access networks: Issues and challenges," *IEEE Netw.*, vol. 30, no. 4, pp. 46–53, Jul. 2016.

[12] D. Boviz, C. S. Chen, and S. Yang, "Effective design of multi-user reception and fronthaul rate allocation in 5G cloud ran," *IEEE J. Sel. Areas Commun.*, vol. 35, no. 8, pp. 1825–01836, Jun. 2017.

[13] M. Xu, F. Lu, J. Wang, L. Cheng, D. Guidotti, and G.-K. Chang, "Key technologies for next-generation digital RoF mobile fronthaul with statistical data compression and multiband modulation," *J. Lightw. Technol.*, vol. 35, no. 17, pp. 3671–3679, Sep. 1, 2017.

[14] M. Sung, S. Cho, H. Chung, S. Kim, and J. Lee, "Investigation of transmission performance in multi-IFoF based mobile fronthaul with dispersion-induced intermixing noise mitigation," *Opt. Exp.*, vol. 25, no. 8, pp. 9346–9357, 2017.

[15] Y. Tian, S. Song, K. Powell, K.-L. Lee, C. Lim, A. Nirmalathas, and X. Yi, "A 60-GHz radio-over-fiber fronthaul using integrated microwave photonics filters," *IEEE Photon. Technol. Lett.*, vol. 29, no. 19, pp. 1663–1666, Oct. 1, 2017.

[16] Y. Li, K. Satyanarayana, M. El-Hajjar, and L. Hanzo, "Analogue radio over fiber aided MIMO design for the learning assisted adaptive C-RAN downlink," *IEEE Access*, vol. 7, pp. 21359–21371, 2019.

[17] K. Zeb, X. Zhang, and Z. Lu, "High capacity mode division multiplexing based mimo enabled all-optical analog millimeter-wave over fiber fronthaul architecture for 5g and beyond," *IEEE Access*, vol. 7, pp. 89533–895220, 2019.

[18] M. Jinno, H. Takara, B. Kozicki, Y. Tsukishima, Y. Sone, and S. Matsuoka, "Spectrum-efficient and scalable elastic optical path network: Architecture, benefits, and enabling technologies," *IEEE Commun. Mag.*, vol. 47, no. 11, pp. 66–73, Nov. 2009.

[19] M. N. S. H. Oliveira and L. S. N. da Fonseca, "P-cycle protected multipath routing, spectrum and core allocation in SDM elastic optical networks," in *Proc. IEEE Int. Conf. Commun. (ICC)*, May 2019, pp. 1–6.

[20] W. Lu, J. Kong, L. Liang, S. Liu, and Z. Zhu, "How much can flexible Ethernet and elastic optical networking benefit mutually," in *Proc. IEEE Int. Conf. Commun. (ICC)*, May 2019, pp. 1–6.

[21] J. Zhao and S. Subramaniam, "Virtual network mapping in elastic optical networks with advance reservation," in *Proc. IEEE Int. Conf. Commun. (ICC)*, Jun. 2020, pp. 1–7.

[22] Y. Liu, H. Gu, F. Yan, X. Yu, and K. Wang, "Multi-controller placement based on two-sided matching in inter-datacenter elastic optical networks," in *Proc. IEEE Int. Conf. Commun. (ICC)*, Jun. 2020, pp. 1–6.

[23] J. Yu, X. Li, and W. Zhou, "Tutorial: Broadband fiber-wireless integration for 5G+ communication," *APL Photon.*, vol. 3, no. 11, Nov. 2018, Art. no. 111101.

[24] M. Kobayashi, R. Murakami, K. Kizaki, S. Saruwatari, and T. Watanabe, "Wireless full-duplex medium access control for enhancing energy efficiency," *IEEE Trans. Green Commun. Netw.*, vol. 2, no. 1, pp. 205–221, Mar. 2018.

[25] *40-Gigabit-Capable Passive Optical Networks (NG-PON2): General Requirements*, International Telecommunication Union, Geneva, Switzerland, Mar. 2013.

[26] *Maxim Integrated*, document MAX2830 Datasheet, 2011.

[27] *ARS Series Datasheet*, Panasonic Electric Works, Osaka, Japan, 2019.

[28] C.-H. Lee, W. V. Sorin, and B. Y. Kim, "Fiber to the home using a PON infrastructure," *J. Lightw. Technol.*, vol. 24, no. 12, pp. 4568–4583, Dec. 2006.

[29] *Gigabit-Capable Passive Optical Networks (GPON): Long Reach*, International Telecommunication Union, Geneva, Switzerland, Nov. 2010.

[30] S. Deronne, V. Moeyaert, and S. Bette, "Analysis of the MAC performances in 802.11g radio-over-fiber systems," in *Proc. 18th IEEE Symp. Commun. Veh. Technol. Benelux (SCVT)*, Nov. 2011, pp. 1–5.

[31] *IEEE Standard for Information Technology—Telecommunications and Information Exchange Between Systems Local and Metropolitan Area Networks—Specific Requirements—Part 11: Wireless Lan Medium Access Control (MAC) and Physical Layer (PHY) Specifications*, Standard 802.11-2016 (Revision IEEE Std 802.11-2012), 2016, pp. 1–3534.

[32] K. Funabiki, T. Nishio, M. Morikura, K. Yamamoto, D. Murayama, and K. Nakahira, "ATRAS: Adaptive MAC protocol for efficient and fair coexistence between radio over fiber-based and CSMA/CA-based WLANs," *EURASIP J. Wireless Commun. Netw.*, vol. 2017, no. 1, pp. 1–13, Jul. 2017.

**TAKUMASA ISHIOKA** (Member, IEEE) received the B.E. and M.E. degrees from Osaka University, Japan, in 2019 and 2021, respectively. His research interest includes wireless networks. He is a member of IPSJ.

**KAZUKI AIURA** received the B.E. degree from Osaka University, Japan, in 2020. His research interest includes wireless networks. He is a member of IPSJ.

**RYOTA SHIINA** received the M.E. degree in material science and engineering from the Tokyo Institute of Technology, Tokyo, Japan, in 2014. In 2014, he joined the NTT Access Network Service Systems Laboratories, where he has been engaged in research on optical access systems mainly related to optical video distribution systems, optical radio-over-fiber transmission systems, and optical wireless communication systems. He received the Young Researcher's Award from the Institute of Electronics, Information, and Communication Engineers (IEICE) of Japan, in 2018, and the Encouraging Award from IEICE Technical Committee on Communication Systems (CS), in 2017. He is a member of IEICE.

**TATSUYA FUKUI** received the B.E. and M.E. degrees from the Faculty of Science and Engineering, Waseda University, Japan, in 2008 and 2010, respectively. He is currently working with the NTT Access Network Service Systems Laboratories. His research interest includes research and development of carrier networks, such as wide-area Ethernet systems.

**TOMOHIRO TANIGUCHI** received the B.E. and M.E. degrees in precision engineering from The University of Tokyo, Tokyo, Japan, in 2000 and 2002, respectively, and the Ph.D. degree in electrical, electronic, and information engineering from Osaka University, Osaka, Japan, in 2010. In 2002, he joined the NTT Access Network Service Systems Laboratories, where he has been engaged in research on optical access systems mainly related to optical heterodyne technologies, radio-on-fiber transmission, and video distribution systems.

**SATOSHI NARIKAWA** received the M.E. and Ph.D. degrees in electronic materials science and engineering from the Faculty of Engineering, Tokyo Institute of Technology, Japan, in 2001 and 2003, respectively. He is currently working with the NTT Access Network Service Systems Laboratories. His research interests include research and development of optical access systems and wide-area Ethernet systems. He received the Academic Encouragement Award of the Society and the Best Paper Award from the Communications Society of Japan.

**KATSUYA MINAMI** received the B.E., M.E., and Ph.D. degrees from Osaka University, Japan, in 1998, 2000, and 2003, respectively. He is currently working with the NTT Access Network Service Systems Laboratories. His research interests include research and development of optical access systems and wide-area Ethernet systems.

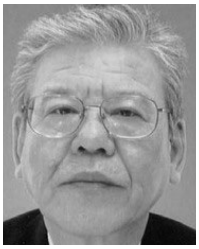

**KAZUHIRO KIZAKI** was with Mitsubishi Electric Corporation, from 1970 to 2004; ATR-Waves Inc., from 2004 to 2006; and Tsuryo Technica Corporation, from 2004 to 2017. He is currently a Researcher with the Graduate School of Information Science and Technology, Osaka University. His research interests include information networks and communications engineering.

**TAKUYA FUJIHASHI** (Member, IEEE) received the B.E. and M.S. degrees from Shizuoka University, Japan, in 2012 and 2013, respectively, and the Ph.D. degree from the Graduate School of Information Science and Technology, Osaka University, Japan, in 2016. He was a Research Fellow (PD) of Japan Society for the Promotion of Science, in 2016. From 2014 to 2015, he was an intern with the Mitsubishi Electric Research Laboratories (MERL). From 2014 to 2016, he was a Research Fellow (DC1) of Japan Society for the Promotion of Science. He is working with the Electronics and Communications Group. He has been an Assistant Professor with the Graduate School of Information Science and Technology, Osaka University, since April 2019. His research interest includes video compression and communications, with a focus on immersive video coding and streaming.

**TAKASHI WATANABE** (Member, IEEE) received the B.E., M.E., and Ph.D. degrees from Osaka University, Japan, in 1982, 1984, and 1987, respectively. He joined the Faculty of Engineering, Tokushima University, as an Assistant Professor, in 1987, and the Faculty of Engineering, Shizuoka University, in 1990. He was a Visiting Researcher with the University of California, Irvine, USA, from 1995 to 1996. He is currently a Professor with the Graduate School of Information Science and Technology, Osaka University. His research interests include mobile networking, ad hoc networks, sensor networks, ubiquitous networks, intelligent transport systems, and MAC and routing. He is a member of IEEE Communications Society, IEEE Computer Society, IPSJ, and IEICE. He has served on many program committees for networking conferences, such as IEEE, ACM, IPSJ, and the Institute of Electronics, Information and Communication Engineers (IEICE), Japan.

**SHUNSUKE SARUWATARI** (Member, IEEE) received the Dr.Sci. degree from The University of Tokyo, in 2007. From 2007 to 2008, he was a Visiting Researcher with the Illinois Genetic Algorithm Laboratory, University of Illinois at Urbana-Champaign. From 2008 to 2012, he was a Research Associate with RCAST, The University of Tokyo. From 2012 to 2016, he was an Assistant Professor with Shizuoka University. He has been an Associate Professor with Osaka University, since 2016. His research interests include wireless networks, sensor networks, and system software.